Journal of the American College of Cardiology Vol. 57, No. 11, 2011

ISSN 0735-1097/$36.00
doi:10.1016/j.jacc.2010.09.072

Can Differences in Corrected Coronary Opacification Measured With Computed Tomography Predict Resting Coronary Artery Flow?

Benjamin J. W. Chow, MD,*† Malek Kass, MD,* Owen Gagné,* Li Chen, MSc,‡ Yeung Yam, BSc,* Alexander Dick, MD,*† George A. Wells, PhD‡

Ottawa, Ontario, Canada

Objectives A proof-of-concept study was undertaken to determine whether differences in corrected coronary opacification (CCO) within coronary lumen can identify arteries with abnormal resting coronary flow.

Background Although computed tomographic coronary angiography can be used for the detection of obstructive coronary artery disease, it cannot reliably differentiate between anatomical and functional stenoses.

Methods Computed tomographic coronary angiography patients (without history of revascularization, cardiac transplantation, and congenital heart disease) who underwent invasive coronary angiography were enrolled. Attenuation values of coronary lumen were measured before and after stenoses and normalized to the aorta. Changes in CCO were calculated, and CCO differences were compared with severity of coronary stenosis and Thrombolysis In Myocardial Infarction (TIMI) flow at the time of invasive coronary angiography.

Results One hundred four coronary arteries (n = 52, mean age = 60.0 ± 9.5 years; men = 71.2%) were assessed. Compared with normal arteries, the CCO differences were greater in arteries with computed tomographic coronary angiography diameter stenoses ≥50%. Similarly, CCO differences were greater in arteries with TIMI flow grade <3 (0.406 ± 0.226) compared with those with normal flow (TIMI flow grade 3) (0.078 ± 0.078, $p < 0.001$). With CCO differences, abnormal coronary flow (TIMI flow grade <3) was identified with a sensitivity and specificity, positive predictive value, and negative predictive value of 83.3% (95% confidence interval [CI]: 57.7 to 95.6%), 91.2% (95% CI: 75.2% to 97.7%), 83.3% (95% CI: 57.7% to 95.6%), and 91.2% (95% CI: 75.2% to 97.7%), respectively. Accuracy of this method was 88.5% with very good agreement (kappa = 0.75, 95% CI: 0.55 to 0.94).

Conclusions Changes in CCO across coronary stenoses seem to predict abnormal (TIMI flow grade <3) resting coronary blood flow. Further studies are needed to understand its incremental diagnostic value and its potential to measure stress coronary blood flow. (J Am Coll Cardiol 2011;57:1280–8) © 2011 by the American College of Cardiology Foundation

Computed tomographic coronary angiography (CTA) is a noninvasive anatomical tool capable of detecting obstructive coronary artery disease (CAD) (1–6). However, a well-recognized limitation of anatomical imaging with CTA is its limited ability to predict the hemodynamic significance of coronary stenoses (7–15). There is a desire to develop a single imaging modality with the ability to evaluate for both anatomical and functional stenoses. Although computed tomography (CT) myocardial perfusion imaging has the potential to assess the hemodynamic significance of an anatomical lesion, it is currently under investigation and is not ready for routine clinical use (16,17).

See page 1289

Opacification of coronary artery lumen and luminal contrast density with CTA is dependent upon contrast bolus geometry (contrast iodine concentration, contrast infusion rate, and volume), timing of image acquisition, cardiac output, and coronary flow. Previous studies using

From the *Division of Cardiology, University of Ottawa Heart Institute, Ottawa, Ontario, Canada; †Department of Radiology, University of Ottawa Heart Institute and The Ottawa Hospital, Ottawa, Ontario, Canada; and the ‡Cardiovascular Research Methods Centre, University of Ottawa Heart Institute, Ottawa, Ontario, Canada. This study was supported in part by the Imaging for Cardiovascular Therapeutics Project #RE02-038 and the Canada Foundation for Innovation #11966. Dr. Chow is supported by Canadian Institutes of Health Research New Investigator Award #MSH-83718; he receives research and fellowship training support from GE Healthcare, Pfizer, and AstraZeneca; fellowship training support from GE Healthcare; and educational support from TeraRecon, Inc. Neither GE Healthcare nor TeraRecon, Inc., was involved in the conduct of the study. All other authors have reported that they have no relationships to disclose.

Manuscript received June 4, 2010; revised manuscript received July 28, 2010, accepted September 14, 2010.

320-detector row CT demonstrate that measuring contrast gradients is feasible and are minimally impacted by these factors (18,19). However, these factors might be an important limitation when evaluating CTA images that are acquired with multiple cardiac cycles and lack temporal uniformity. If methods could be developed to partially correct for such factors, 64-slice CT might be able to measure coronary contrast opacification to indirectly estimate coronary blood flow. This technique might prove especially useful for estimating flow across unevaluable coronary segments, such as stents, which might improve diagnostic accuracy. Equally valuable would be the ability to translate this method to facilitate the measure of stress coronary flow allowing for the determination of hemodynamically significant stenoses.

The objective of this proof-of-concept study is to determine whether changes in corrected coronary opacification (CCO) across stenoses can identify arteries with abnormal resting coronary flow.

Methods

Consecutive patients who had undergone routine CTA and subsequent invasive coronary angiography, were retrospectively screened for analysis. All patients with a history of coronary revascularization, cardiac transplantation, and congenital heart disease were excluded. The Cardiac CT registry was approved by the Institutional Human Research Ethics Board, and all patients provided written informed consent.

CTA. Before image acquisition, metoprolol or diltiazem (oral and/or intravenous) was administered targeting a heart rate of ≤65 beats/min, and nitroglycerin 0.8 mg was administered sublingually. A bi-phasic timing bolus was used to determine the time interval between intravenous contrast (Visipaque 320 or Omnipaque 350, GE Healthcare, Princeton, New Jersey) infusion and peak aorta opacification (6,20). As per our clinical routine, final images were acquired with a tri-phasic intravenous contrast administration protocol (100% contrast, 40%/60% contrast/saline, and saline [40 cc]) (6,20). No modifications were made to the CTA protocol for the purpose of this study. Retrospective electrocardiogram (ECG)-gated datasets were acquired with the GE Volume CT (GE, Milwaukee, Wisconsin) with 64 × 0.625 mm slice collimation, gantry rotation of 350 ms (mA = 400 to 800, kV = 120) with ECG-gated X-ray tube modulation and pitch (0.16 to 0.24) was individualized according to the heart rate of the patient. The CTA datasets were reconstructed with a slice thickness of 0.625 mm and an increment of 0.4 mm with the cardiac phase(s) with the least cardiac motion (6,20).

CTA image analysis. The ECG-gated CT images were post-processed with the GE Advantage Volume Share Workstation and interpreted by expert observers blinded to all clinical data. A 17-segment model of the coronary arteries and obstructive CAD was defined as a diameter stenosis ≥50% (6,20,21).

For each patient, a single expert observer measured coronary luminal attenuation values (Hounsfield units [HU]) in normal arteries and those with obstructive CAD (≥50% diameter stenosis) on CTA. Once a coronary segment(s) was selected for analysis, the axial slice (0.625-mm slice thickness) that approximated the center of the lumen in the z-plane (estimated by selecting the axial slice with the largest luminal diameter in the x-y plane) was used for analysis. A region of interest (ROI) was placed in the center of the coronary lumen (x-y plane) and the descending aorta (on the same axial slice) (Fig. 1), and the mean HU values were recorded. The largest possible ROI was used; however, care was used when placing the ROI to ensure that all extra-luminal structures (e.g., plaque) and artefact were excluded. At least 4 ROI measurements were made for all normal arteries with proximal, mid, and distal coronary segments. In arteries with obstructive CAD, a minimum of 6 ROIs were placed. At least 2 ROI measurements were performed proximal to the stenosis, 2 measurements were performed immediately distal to the stenosis (within 2 cm of the lesion), and 2 measurements were performed in the distal artery with a diameter ≥1.5 mm. Care was also used to place ROIs in segments of the artery without significant artefact (motion, beam hardening, or blooming artefact).

For training purposes and to determine inter- and intra-observer variability, the attenuation values of the aorta and

Abbreviations and Acronyms

- **CAD** = coronary artery disease
- **CCO** = corrected coronary opacification
- **CI** = confidence interval
- **CT** = computed tomography
- **CTA** = computed tomographic coronary angiography
- **ECG** = electrocardiogram
- **HU** = Hounsfield units
- **ICC** = intra-class correlation coefficient
- **IQR** = interquartile range
- **MI** = myocardial infarction
- **ROI** = region of interest
- **TIMI** = Thrombolysis In Myocardial Infarction

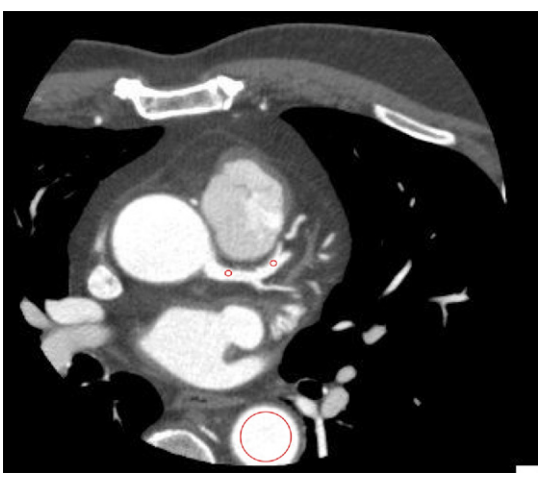

Figure 1 Regions of Interest Used for Calculating the Corrected Coronary Opacification

Regions of interest placed in the left main and proximal left anterior descending artery **(small red circles)** and in the descending aorta **(large red circle)**.

coronary arteries were measured by 2 expert readers in 15 nonstudy patients.

Patients were excluded from analysis if they had left main or ostial right coronary artery stenoses (n = 4), serial stenoses (n = 10), or branch vessel disease (n = 7). As well, 14 patients without a "normal" reference major epicardial vessel were excluded, as were patients with coronary segments with significant artefact (cardiac motion [n = 9], beam hardening artefact [n = 4]) or vessels with diameters <1.5 mm (n = 14).

CCO. It is accepted that there are normal variations in the opacification of the coronary arteries (18,19); however, this variability is likely greater when image acquisition occurs over multiple cardiac cycles (Fig. 2). To account for variations in contrast attenuation in the coronary vessels due to different cardiac cycles, cardiac output, and bolus geometry, each coronary luminal attenuation measurement was normalized to the descending aorta on the same axial slice. Thus, for each axial slice, the corrected coronary attenuation (CCO) was calculated as the quotient of the mean ROI HU in the coronary artery and aorta (CCO = coronary artery HU/aorta HU). The difference in CCO across stenoses was calculated as the change between the lowest CCO proximal to the stenosis and the lowest CCO distal to the coronary stenosis (CCO difference = pre-stenosis CCO_{min} − post-stenosis CCO_{min}). Normal arteries were used to measure the variability of CCO and were calculated as the difference between the highest and the lowest CCO (CCO_{max} − CCO_{min}) within the same coronary artery.

Invasive coronary angiography. Invasive coronary angiography was performed at the discretion of the treating physician, and cinematic images were acquired with a frame rate of 15 frames/s. With the same 17-segment model of the coronary arteries, percentage diameter stenosis of each artery was assessed (6,20,21). In addition, TIMI flow grade (TIMI flow grade 0, 1, 2, or 3) and the TIMI frame count were calculated for each artery of interest. The TIMI frame count (30 frames/s) was calculated by doubling the count acquired with the 15 frames/s cinematic images (22).

Statistical analysis. Statistical analyses were performed with SAS (version 9.2, SAS Institute, Inc., Cary, North Carolina), and statistical significance was defined as $p < 0.05$. Continuous variables were presented as means with SDs and median (interquartile range [IQR]), and categorical variables were presented as frequencies with percentages. To compare patient characteristics, Wilcoxon rank sum test was used to compare continuous variables, and Fisher exact test was used for categorical variables.

The unpaired *t* tests were used to compare the difference of CCO gradients between normal versus obstructive arteries and between normal (TIMI flow grade 3) and abnormal (TIMI flow grade <3) coronary flow. Paired *t* tests were used to compare differences in coronary flow, CCO gradients, and TIMI frame counts versus coronary diameter stenosis. The reliability of continuous data (CCO gradient, coronary flow, TIMI frame count versus coronary diameter stenosis, inter- and intra-observer variability) was assessed with intra-class correlation coefficients (ICCs) (23). The strength of ICC was determined with the cutoffs of 0.5, 0.3, and 0.1 for high, moderate, and low levels of agreement according to Cohen's effect size convention (24). The agreement between abnormal CCO gradients and coronary flow (TIMI flow grade <3) was evaluated with Kappa statistics.

Results

An obstructive and a nonobstructive vessel were assessed for each of the 52 consecutive patients (mean age 60.0 ± 9.5 years;

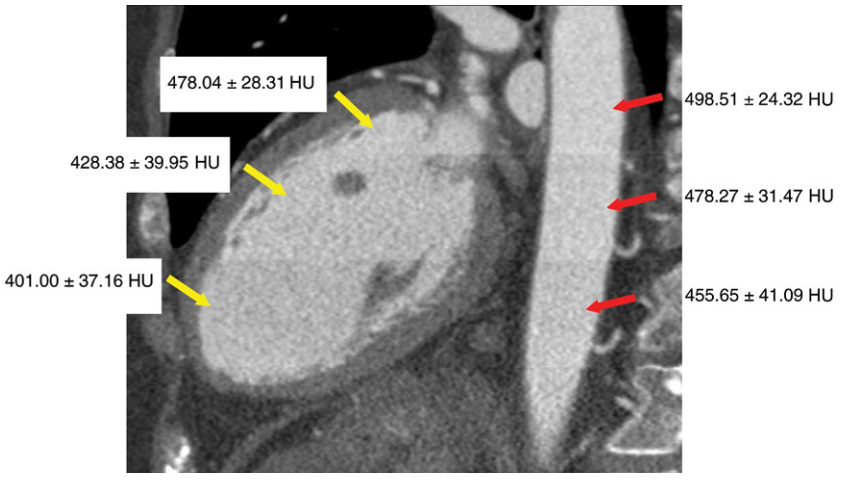

Figure 2 Contrast Variability Due to the Lack of Temporal Uniformity of 64-Slice CT

Contrast enhanced electrocardiographic-gated cardiac computed tomography (CT) with varying contrast density (Hounsfield units [HU]) in the aorta **(red arrows)** and left ventricle **(yellow arrows)**, suggesting that the opacification of vascular structures is nonuniform when image acquisition spans multiple cardiac cycles.

Table 1 Patient Characteristics: All Patients and Patients With and Without TIMI Flow Grade 3

	All Patients (n = 52)	TIMI Flow Grade = 3 (n = 34)	TIMI Grade <3 (n = 18)	p Value*
Age (yrs)	60.0 ± 9.5	59.6 ± 9.1	60.7 ± 10.4	0.700
Men	37 (71.2%)	24 (70.6%)	13 (72.2%)	0.902
Body mass index (kg/m^2)	29.7 ± 5.7	30.7 ± 5.8	27.9 ± 5.2	0.102
Pre-test likelihood for CAD (%)	52.4 ± 35.8	53.1 ± 37.4	51.1 ± 33.8	0.847
Cardiac risk factors				
Smoker/ex-smoker	30 (57.7%)	17 (50.0%)	13 (72.2%)	0.126
Hypertension	29 (55.8%)	19 (55.9%)	10 (55.6%)	0.982
Dyslipidemia	37 (71.2%)	25 (73.5%)	12 (66.7%)	0.607
Diabetes	11 (21.2%)	8 (23.5%)	3 (16.7%)	0.568
Family history of CAD	29 (55.8%)	21 (61.8%)	8 (44.4%)	0.236
Indications for study				
Chest pain	36 (69.2%)	25 (73.5%)	11 (61.1%)	0.361
Nonanginal chest pain	11 (21.2%)	10 (29.4%)	1 (5.6%)	0.047
Atypical angina	14 (26.9%)	6 (17.6%)	8 (44.4%)	0.040
Typical angina	11 (21.2%)	9 (26.5%)	2 (11.1%)	0.201
Dyspnea	8 (15.4%)	4 (11.8%)	4 (22.2%)	0.325
Asymptomatic	8 (15.4%)	5 (14.7%)	3 (16.7%)	0.854
Equivocal stress test	4 (7.7%)	3 (8.8%)	1 (5.6%)	0.677
Cardiac (valve) surgery	1 (1.9%)	1 (2.9%)	0 (0.0%)	0.467
Risk stratification	3 (5.8%)	1 (2.9%)	2 (11.1%)	0.234
CT imaging parameters				
Imaging heart rate (beats/min)	53.6 ± 5.7	55.1 ± 5.3	50.9 ± 5.6	0.010
Contrast infusion rate (cc/s)	6.3 ± 0.8	6.4 ± 0.8	6.3 ± 0.8	0.746
Total contrast volume (cc)	104.2 ± 12.8	105.0 ± 14.2	102.7 ± 9.6	0.541
Radiation (mSv)	15.6 ± 3.3	15.8 ± 3.8	15.2 ± 2.2	0.561

Values are mean ± SD or n (%). *Comparison between patients with Thrombolysis In Myocardial Infarction (TIMI) flow grade 3 (column 3) and those with TIMI flow grade <3 (column 4).

CAD = coronary artery disease; CT = computed tomography.

71.2% male) (Table 1). All patients had obstructive CAD in ≥1 vessel and all patients had at least 1 major epicardial vessel that could be used as a "normal" reference artery. Of the 884 segments evaluated, 55 (6.2%) were <1.5 mm in diameter, and 26 (2.9%) were unevaluable due to artefact.

Normal arteries. The CCO was assessed in 52 coronary arteries without stenoses and normal TIMI flow grade 3 (20 left anterior descending arteries, 24 circumflex arteries, and 8 right coronary arteries). In normal arteries, the mean CCO was 0.979 ± 0.070 (median 0.965, IQR: 0.940 to 1.005), CCO_{max} was 1.030 ± 0.076 (median 1.020, IQR: 0.987 to 1.057), and CCO_{min} was 0.921 ± 0.093 (median 0.926, IQR: 0.892 to 0.954). To estimate normal variability in arteries without coronary stenosis, normal CCO variability (difference between CCO_{max} and CCO_{min}) was calculated (0.100 ± 0.042) (median 0.099, IQR: 0.073 to 0.128). The CCO variability in normal arteries was used to calculate the threshold for abnormal CCO differences (mean CCO difference + 2 SD = 0.184). Therefore a CCO difference (pre-stenosis CCO_{min} − post-stenosis CCO_{min}) >0.184 was considered abnormal, and this threshold was tested in coronary arteries with varying stenoses, TIMI flow grade, and TIMI frame count.

Validation in arteries with diameter stenoses ≥50%. The CCO was measured in 52 obstructive arteries with CTA diameter stenoses ≥50% (23 left anterior descending arteries, 5 circumflex arteries, and 24 right coronary arteries). The pre-stenosis CCO_{min} (0.964 ± 0.058, median 0.958, IQR: 0.926 to 0.994) was slightly greater than CCO_{min} in normal arteries (0.921 ± 0.093, median 0.926, IQR: 0.892 to 0.954) ($p = 0.006$). The post-stenosis CCO_{min} (0.773 ± 0.214, median 0.866, IQR: 0.683 to 0.916) were significantly lower than the minimum pre-stenosis CCO_{min} ($p < 0.001$) and lower than the CCO_{min} observed in normal arteries ($p < 0.001$).

Compared with the CCO variability in nonobstructive arteries, the CCO difference was significantly greater in arteries with obstructive CAD (diameter stenoses ≥50%) (0.191 ± 0.214, median 0.106, IQR: 0.042 to 0.296) ($p = 0.004$) (Fig. 3).

The relationship between CCO differences and coronary diameter stenoses was also assessed (Table 2), and the proportion of abnormal CCO differences increased with worsening diameter stenosis ($p < 0.001$). According Cohen's effect size convention, the reliability of contrast gradient and coronary diameter stenosis was high (ICC: 0.82; 0.71 to 0.89).

TIMI flow grade <3. In arteries with abnormal coronary flow (TIMI flow grade <3), the mean pre-stenosis CCO and CCO_{min} were 1.000 ± 0.075 and 0.970 ± 0.067, respectively, and were similar to the measures obtained in

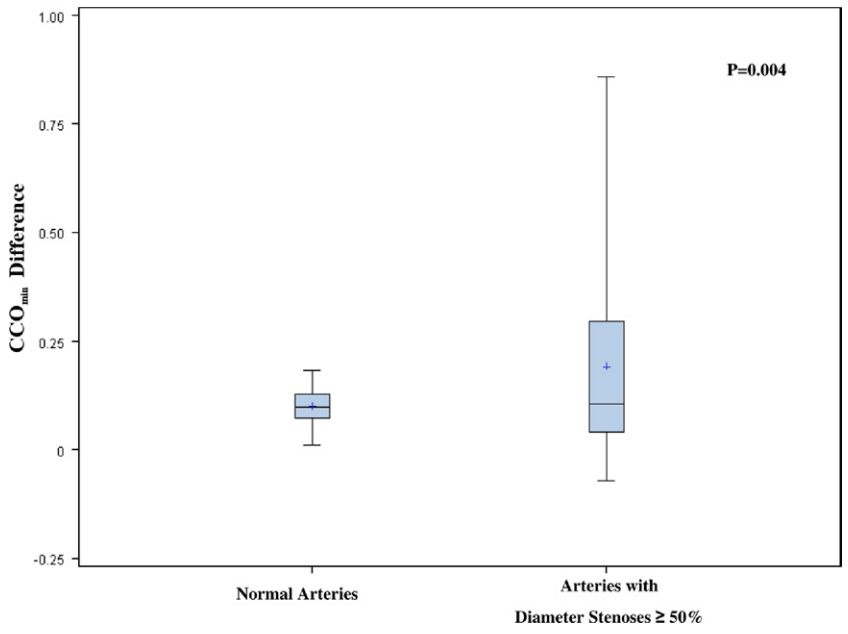

Figure 3 Comparison of CCO in Arteries With and Without Obstructive Coronary Artery Disease

Box whisker plot of corrected coronary opacification $(CCO)_{min}$ differences between normal arteries and arteries with diameter stenoses ≥50% (p = 0.004) + = mean; − = median; upper tail = maximum; lower tail = minimum.

arteries with normal TIMI flow grade 3 (0.987 ± 0.057 and 0.961 ± 0.054, respectively; p = NS) (Table 3).

However, CCO differences in arteries with TIMI flow grade <3 (0.406 ± 0.226) were significantly higher than those with normal TIMI flow grade 3 (0.078 ± 0.078; p < 0.001) and normal arteries (0.100 ± 0.042; p < 0.001) (Table 3, Fig. 4).

With the threshold >0.184, abnormal coronary flow (TIMI flow grade <3) was identified with a sensitivity and specificity, positive predictive value, and negative predictive value of 83.3% (95% CI: 57.7 to 95.6%), 91.2% (95% CI: 75.2 to 97.7%), 83.3% (95% CI: 57.7 to 95.6%), and 91.2% (95% CI: 75.2 to 97.7%), respectively (Table 4). Accuracy of this method was 88.5% with very good agreement (kappa = 0.75 [95% CI: 0.55 to 0.94]. Two patients with severe coronary stenosis but with different TIMI flow grade 3 (Fig. 5A) and TIMI flow grade <3 (Fig. 5B) are shown.

The relationships among TIMI flow grade, TIMI frame count, and coronary diameter stenosis were also assessed (Table 2). As expected, the proportion of abnormal coronary flow (TIMI flow grade <3) and TIMI frame counts increased with worsening diameter stenosis (p < 0.001 and p < 0.001, respectively). The reliability of TIMI frame count versus coronary diameter stenosis and TIMI frame count versus CCO differences were similar (ICC: 0.52, 0.27 to 0.71 and 0.55, 0.30 to 0.73, respectively).

Uncorrected coronary opacification. Coronary opacification was corrected to the aorta, recognizing that image acquisition is not temporally uniform and occurs over several cardiac cycles. To better understand the importance of this normalization (CCO), the analysis was performed with the "uncorrected" coronary opacification attenuation values.

Coronary opacification was assessed in the same 52 coronary arteries without stenoses and normal TIMI flow

Table 2 Relationships Among Diameter Stenosis and TIMI Flow Grade, TIMI Frame Count, and CCO Gradients Vessels With Obstructive CAD

	CAD (Diameter Stenosis)					
	<50%	50%–69%	70%–89%	90%–99%	100%	p Value
TIMI flow grade 3	7 (100.0%)	7 (100.0%)	10 (100.0%)	10 (66.7%)	0	<0.001
TIMI flow grade 0, 1, or 2	0	0	0	5 (33.3%)	13 (100.0%)	
TIMI frame count	25.3 ± 9.4 (16.0–34.0)	27.3 ± 7.3 (22.0–35.0)	31.4 ± 16.3 (24.0–34.0)	39.3 ± 22.3 (24.0–51.0)	66.0 ± 36.4 (40.0–96.0)	<0.001
Normal CCO gradient	7 (100.0%)	6 (85.7%)	9 (90.0%)	12 (80.0%)	0	<0.001
Abnormal CCO gradient (>0.184)	0	1 (14.3%)	1 (10.0%)	3 (20.0%)	13 (100.0%)	

Values are n (%) or mean ± SD (interquartile range). n = 52 vessels.
CAD = coronary artery disease; CCO = corrected coronary opacification; TIMI = Thrombolysis In Myocardial Infarction.

Table 3 CCO in Patients With Abnormal Resting Coronary Blood Flow

	TIMI Flow Grade <3	TIMI Flow Grade 3	Normal Artery	p Value
Pre-stenosis CCO_{mean}				NS
Mean	1.000 ± 0.075	0.987 ± 0.057		
Median (IQR)	1.000 (0.937–1.032)	0.996 (0.947–1.011)		
Pre-stenosis CCO_{min}				NS
Mean	0.970 ± 0.067	0.961 ± 0.054		
Median (IQR)	0.957 (0.932–0.998)	0.958 (0.921–0.992)		
CCO_{min} difference				<0.001
Mean	0.406 ± 0.226	0.078 ± 0.078	0.100 ± 0.042	
Median (IQR)	0.361 (0.251–0.538)	0.070 (0.025–0.107)	0.099 (0.073–0.128)	

Abbreviations as in Table 2.

grade 3. The maximum and minimum coronary attenuation values were 936.0 ± 608.2 HU (median 517.3 HU, IQR: 424.9 to 1,634.0 HU) and 336.4 ± 108.1 HU (median 352.6 HU, IQR: 285.5 to 414.5 HU), respectively. The variability of coronary attenuation was 599.6 ± 584.4 HU (median 282.5 HU, IQR: 76.4 to 1,266.8 HU).

The relationship between contrast attenuation and coronary diameter stenoses was poor, unlike CCO, and differences in coronary attenuation across coronary stenoses did not increase with worsening diameter stenosis.

A decline in coronary contrast attenuation >1,768 HU was considered abnormal, with the same methodology to calculate the threshold for abnormal (mean + 2 SD). This threshold was not able to identify arteries with obstructive CAD or abnormal resting coronary flow. According Cohen's effect size convention, the reliability of contrast gradient and coronary diameter stenosis was low (ICC: 0.27, 0.00 to 0.50).

Interobserver and intraobserver variability. The reliability of the interobserver of the non-normalized attenuation measures was excellent in the coronary arteries (0.94, 95% CI: 0.896 to 0.966) and the aorta (1.00). Similarly, the intra-observer reliability was equally excellent in the coronary arteries (0.99, 95% CI: 0.982 to 0.994) and aorta (1.00).

Discussion

The ability of CTA to estimate coronary blood flow and to assess for functional coronary stenosis would be extremely desirable. Such a technique might prove to be useful in settings of unevaluable coronary segments, perhaps by improving the diagnostic accuracy of CTA. Equally important would be its potential applicators to measure stress coronary blood flow, thus permitting the assessment of hemodynamic significance

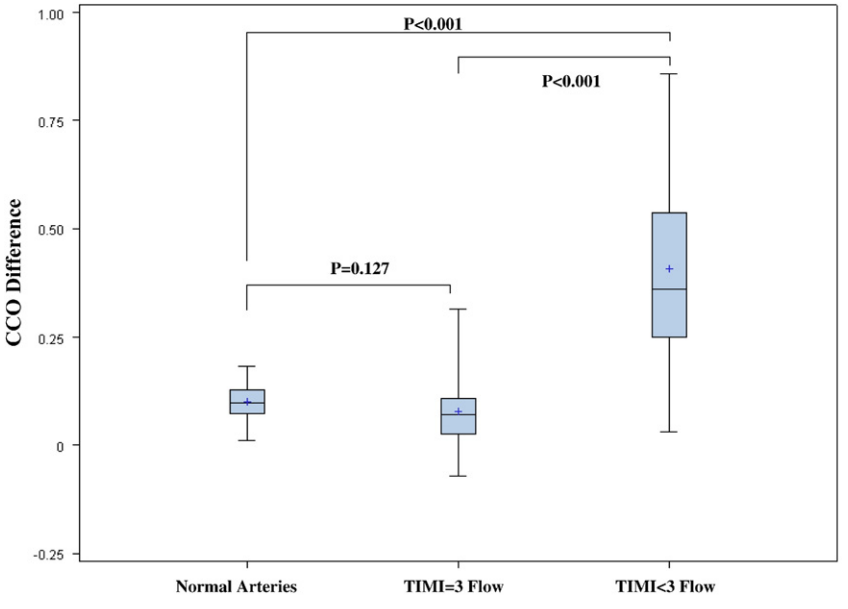

Figure 4 Comparison of CCO in Patients With Normal and Abnormal Resting Flow

Box whisker plot of corrected coronary opacification (CCO) differences among normal arteries (CCO_{max} − CCO_{min}) and abnormal arteries (pre-stenosis CCO_{min} − post-stenosis CCO_{min}), with TIMI flow grade 3 and TIMI flow grade <3 ($p < 0.001$). + = mean; − = median; upper tail = maximum; lower tail = minimum.

Table 4 Abnormal and Normal CCO Gradients

	TIMI Flow Grade <3	TIMI Flow Grade 3
Abnormal CCO gradient	15	3
Normal CCO gradient	3	31

Kappa = 0.75 (0.55–0.94).
CCO = corrected coronary opacification; TIMI = Thrombolysis In Myocardial Infarction.

of a lesion. This proof-of-concept study demonstrates that the agreement and operating characteristics of CCO differences in identifying abnormal (TIMI flow grade <3) resting coronary flow seem to be very good.

Contrast gradients have been studied with 320-detector row CT (18,19). Using a scanner capable of imaging the entire coronary tree within 1 cardiac cycle permits accurate assessment of coronary artery contrast gradients. However, CT scanners with incomplete cardiac coverage that require multiple cardiac cycles for image acquisition lack temporal uniformity and might be further influenced by factors beyond coronary flow. Figure 2 highlights potential changes in contrast opacification during image acquisition, supporting the notion that contrast opacification changes during image acquisition. We hypothesized that changes in coronary opacification might be corrected and normalized to the descending aorta. If true, CCO in "normal" arteries should approach 1.0. The mean CCO in "normal" arteries (0.979 ± 0.070) supports this hypothesis and suggests that CCO might be feasible with

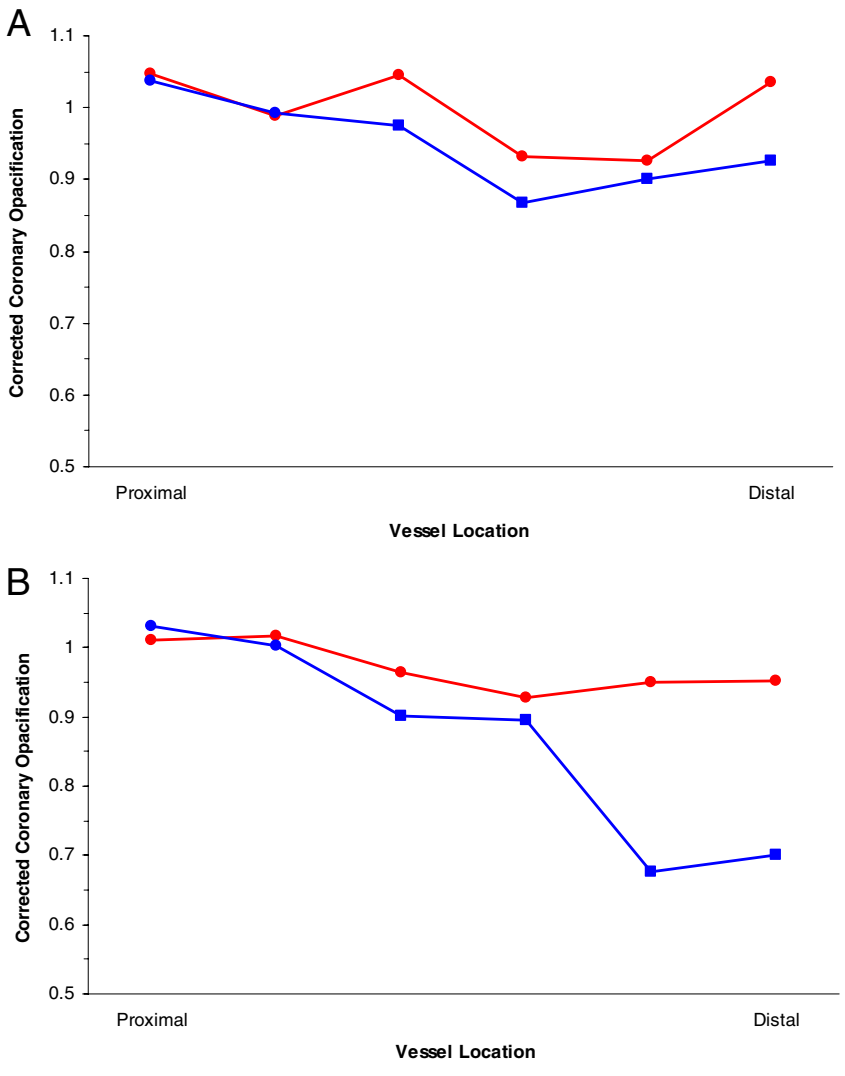

Figure 5 CCO in Patients With Normal and Abnormal Resting Coronary Flow

(A) Corrected coronary opacification (CCO) measures in a coronary artery with 95% stenosis of the right coronary artery **(blue line)** (pre-stenosis **[blue circles]** and post-stenosis **[blue squares]**) with normal flow (Thrombolysis In Myocardial Infarction flow grade 3) and in an artery without coronary stenosis **(red line)**. **(B)** The CCO measures in a coronary artery with 95% stenosis of the left anterior descending coronary artery **(blue line)** (pre-stenosis **[blue circles]** and post-stenosis **[blue squares]**) with abnormal flow (Thrombolysis In Myocardial Infarction flow grade 2) and in an artery without coronary stenosis **(red line)**.

64-slice CT. Most importantly, this technique might be applied to existing CT scanners with incomplete cardiac coverage and might have future application in the assessment of stress coronary blood flow.

To further confirm that correcting coronary opacification to the aorta is justified, the same analyses were performed with the "uncorrected" coronary opacification attenuation values. The results confirm that the uncorrected values could not accurately predict coronary stenoses or abnormal resting coronary flow.

Limitations of anatomical imaging. Previous studies have confirmed that anatomical stenoses poorly predict hemodynamic and functional significance, and this variability seems to be most prevalent in lesions with moderate stenoses (10–12,15,25–27). The importance of determining functional significance has been highlighted in several studies showing that functional assessment has incremental prognostic value over coronary anatomy alone (28,29). Further compounding the limitations of anatomical assessment are the inherent limitations of CTA. Suboptimal temporal resolution, spatial resolution, blooming artefact, and beam-hardening artefact from coronary calcification or stents limit the anatomical accuracy of CTA. Functional assessment of stenoses with CT might have incremental diagnostic and prognostic value, acknowledging the limitations of CTA and anatomical imaging.

Potential applications. At first glance, the ability to measuring CCO differences at rest and the ability to identify abnormal resting coronary flow might seem to have limited value. However, the application of CCO might be useful in patients with unevaluable segments (severe coronary calcification or stents) that reduce the ability of the reader to assess for coronary stenoses. Measuring CCO at rest might not be a sensitive measure of stenosis but could be a specific tool for detecting abnormal flow. More interesting is its potential utility in conjunction with pharmacologic stress. With pharmacologic vasodilator stress, one would expect augmentation of coronary flow in normal arteries, but flow would be attenuated in arteries with fixed stenoses. Comparing changes in CCO between normal and abnormal arteries might prove to accurately measure functional stenoses.

Study limitations. This was a single-center retrospective analysis of a prospectively enrolled cohort. Although small, the results are encouraging but require further study and validation in larger cohorts. As well, further study is needed to understand its incremental value and its potential utility in conjunction with CT stress imaging. Similarly, further understanding is needed to determine whether such methods might be generalized to different contrast administration protocols.

The authors recognize that a more rigorous analysis of CCO might have been achieved with fixed-interval ROI HU measurements extending the entire coronary tree, as previously done by Steigner et al. (18). In our study, the limitation of image acquisition spanning multiple cardiac cycles required that coronary contrast opacification be normalized to the aorta on the corresponding axial slice. As such, automated curved multiplanar reformation software could not be used to perform HU measurements. Because our aim was to devise a simple method that could be easily applied in clinical practice, we minimized CCO measures to ensure clinical feasibility. At least 6 measures were obtained, 2 pre- and 4 post-stenoses ROIs were placed with axial slices obtained during different cardiac cycles. A simple calculation (pre-stenosis CCO_{min} − post-stenosis CCO_{min}) seems to identify abnormal resting coronary blood flow.

The calculation of CCO requires the accurate measurement of coronary opacification and is potentially limited by image quality (signal/noise ratio), vessel size, beam hardening or blooming artefact, and partial volume. Although our initial results are promising, further study is needed to fully comprehend its clinical potential.

Conclusions

Changes in CCO in coronary vessels might predict resting coronary blood flow. Further studies are needed to understand its incremental value and its potential utility to measure stress coronary blood flow.

Acknowledgments

The authors extend their gratitude to Kathryn Callidine, Nancy Chow, Micheala Garkish, Debbie Gauthier, Patricia Grant, Sandina Jamieson, and Richard Tessier for their expertise and dedication to Cardiac CT Research.

Reprint requests and correspondence: Dr. Benjamin J. W. Chow, University of Ottawa Heart Institute, 40 Ruskin Street, Ottawa, Ontario K1Y 4W7, Canada. E-mail: bchow@ottawaheart.ca.

REFERENCES

1. Chow BJ, Hoffmann U, Nieman K. Computed tomographic coronary angiography: an alternative to invasive coronary angiography. Review article. Can J Cardiol 2005;21:933–40.
2. Beanlands RS, Chow BJ, Dick A, et al. CCS/CAR/CANM/CNCS/CanSCMR joint position statement on advanced noninvasive cardiac imaging using positron emission tomography, magnetic resonance imaging and multidetector computed tomographic angiography in the diagnosis and evaluation of ischemic heart disease—executive summary. Can J Cardiol 2007;23:107–19.
3. Vanhoenacker PK, Heijenbrok-Kal MH, Van Heste R, et al. Diagnostic performance of multidetector CT angiography for assessment of coronary artery disease: meta-analysis. Radiology 2007;244:419–28.
4. Abdulla J, Abildstrom SZ, Gotzsche O, Christensen E, Kober L, Torp-Pedersen C. 64-multislice detector computed tomography coronary angiography as potential alternative to conventional coronary angiography: a systematic review and meta-analysis. Eur Heart J 2007;28:3042–50.
5. Hamon M, Biondi-Zoccai GG, Malagutti P, et al. Diagnostic performance of multislice spiral computed tomography of coronary arteries as compared with conventional invasive coronary angiography: a meta-analysis. J Am Coll Cardiol 2006;48:1896–910.
6. Chow BJW, Abraham A, Wells GA, et al. Diagnostic accuracy and impact of computed tomographic coronary angiography on utilization of invasive coronary angiography. Circ Cardiovasc Imag 2009;2:16–23.

7. Chow BJ, Dennie C, Hoffmann U, et al. Comparison of computed tomographic angiography versus rubidium-82 positron emission tomography for the detection of patients with anatomical coronary artery disease. Can J Cardiol 2007;23:801–7.
8. Gaemperli O, Schepis T, Koepfli P, et al. Accuracy of 64-slice CT angiography for the detection of functionally relevant coronary stenoses as assessed with myocardial perfusion SPECT. Eur J Nucl Med Mol Imaging 2007;34:1162–71.
9. Nicol ED, Stirrup J, Reyes E, et al. Sixty-four-slice computed tomography coronary angiography compared with myocardial perfusion scintigraphy for the diagnosis of functionally significant coronary stenoses in patients with a low to intermediate likelihood of coronary artery disease. J Nucl Cardiol 2008;15:311–8.
10. Schuijf JD, Wijns W, Jukema JW, et al. Relationship between noninvasive coronary angiography with multi-slice computed tomography and myocardial perfusion imaging. J Am Coll Cardiol 2006;48:2508–14.
11. Rispler S, Keidar Z, Ghersin E, et al. Integrated single-photon emission computed tomography and computed tomography coronary angiography for the assessment of hemodynamically significant coronary artery lesions. J Am Coll Cardiol 2007;49:1059–67.
12. Meijboom WB, Van Mieghem CAG, van Pelt N, et al. Comprehensive assessment of coronary artery stenoses: computed tomography coronary angiography versus conventional coronary angiography and correlation with fractional flow reserve in patients with stable angina. J Am Coll Cardiol 2008;52:636–43.
13. White CW, Wright CB, Doty DB, et al. Does visual interpretation of the coronary arteriogram predict the physiologic importance of a coronary stenosis? N Engl J Med 1984;310:819–24.
14. Uren NG, Melin JA, de Bruyne B, Wijns W, Baudhuin T, Camici PG. Relation between myocardial blood flow and the severity of coronary-artery stenosis. N Engl J Med 1994;330:1782–8.
15. Hacker M, Jakobs T, Hack N, et al. Sixty-four slice spiral CT angiography does not predict the functional relevance of coronary artery stenoses in patients with stable angina. Eur J Nucl Med Mol Imaging 2007;34:4–10.
16. Okada DR, Ghoshhajra BB, Blankstein R, et al. Direct comparison of rest and adenosine stress myocardial perfusion CT with rest and stress SPECT. J Nucl Cardiol 2010;17:27–37.
17. Blankstein R, Shturman LD, Rogers IS, et al. Adenosine-induced stress myocardial perfusion imaging using dual-source cardiac computed tomography. J Am Coll Cardiol 2009;54:1072–84.
18. Steigner ML, Mitsouras D, Whitmore AG, et al. Iodinated contrast opacification gradients in normal coronary arteries imaged with prospectively ECG-gated single heart beat 320-detector row computed tomography. Circ Cardiovasc Imaging 2010;3:179–86.
19. Rybicki FJ, Otero HJ, Steigner ML, et al. Initial evaluation of coronary images from 320-detector row computed tomography. Int J Cardiovasc Imaging 2008;24:535–46.
20. Chow BJW, Wells GA, Chen L, et al. Prognostic value of 64-slice cardiac computed tomography: severity of coronary artery disease, coronary atherosclerosis and left ventricular ejection fraction. J Am Coll Cardiol 2010;55:1017–28.
21. Hoffmann U, Moselewski F, Cury RC, et al. Predictive value of 16-slice multidetector spiral computed tomography to detect significant obstructive coronary artery disease in patients at high risk for coronary artery disease: patient- versus segment-based analysis. Circulation 2004;110:2638–43.
22. Vijayalakshmi K, Ashton VJ, Wright RA, et al. Corrected TIMI frame count: applicability in modern digital catheter laboratories when different frame acquisition rates are used. Catheter Cardiovasc Interv 2004;63:426–32.
23. Shrout PE, Fleiss JL. Intraclass correlations: uses in assessing rater reliability. Psychol Bull 1979;86:420–8.
24. Cohen J. A power primer. Psychol Bull 1992;112:155–9.
25. Tobis J, Azarbal B, Slavin L. Assessment of intermediate severity coronary lesions in the catheterization laboratory. J Am Coll Cardiol 2007;49:839–48.
26. Christou MA, Siontis GC, Katritsis DG, Ioannidis JP. Meta-analysis of fractional flow reserve versus quantitative coronary angiography and noninvasive imaging for evaluation of myocardial ischemia. Am J Cardiol 2007;99:450–6.
27. Kern MJ, Lerman A, Bech JW, et al. Physiological assessment of coronary artery disease in the cardiac catheterization laboratory: a scientific statement from the American Heart Association Committee on Diagnostic and Interventional Cardiac Catheterization, Council on Clinical Cardiology. Circulation 2006;114:1321–41.
28. Pijls NH, van Schaardenburgh P, Manoharan G, et al. Percutaneous coronary intervention of functionally nonsignificant stenosis: 5-year follow-up of the DEFER Study. J Am Coll Cardiol 2007;49:2105–11.
29. Iskandrian AS, Chae SC, Heo J, Stanberry CD, Wasserleben V, Cave V. Independent and incremental prognostic value of exercise single-photon emission computed tomographic (SPECT) thallium imaging in coronary artery disease. J Am Coll Cardiol 1993;22:665–70.

Key Words: computed tomography ■ coronary angiography ■ coronary occlusion ■ functional stenosis.